

times in the vicinity of the label, plus extra terms, which provide a theoretical way to unravel the contributions from the label and from the ideal chain and to extract the intrinsic chain jump frequency. Besides the experimental difficulties involved in this quantitative approach, the model provides a comprehensive qualitative frame for interpreting presently available experiments. Finally, it is worth noticing that this perturbation approach is not restricted to labeling problems but can be extended to any situation involving inhomogeneities in a polymer chain.

**Acknowledgment.** We are indebted to Pr. L. Monnerie and Pr. E. Helfand for helpful discussions.

## References and Notes

- (1) (a) Valeur, B.; Jarry, J. P.; Geny, F.; Monnerie, L. *J. Polym. Sci., Polym. Phys. Ed.* **1975**, *13*, 667. (b) Valeur, B.; Jarry, J. P.; Geny, F.; Monnerie, L. *J. Polym. Sci., Polym. Phys. Ed.* **1975**, *13*, 675.
- (2) Jones, A. A.; Stockmayer, W. H. *J. Polym. Sci., Polym. Phys. Ed.* **1977**, *15*, 847.
- (3) Bendler, J. T.; Yaris, R. *Macromolecules* **1978**, *11*, 650.
- (4) Hall, C. K.; Helfand, E. *J. Chem. Phys.* **1982**, *77*, 3275.
- (5) Viogy, J. L.; Monnerie, L.; Brochon, J. C. *Macromolecules* **1983**, *16*, 1845.
- (6) Hyde, P. D.; Waldow, D. A.; Ediger, M. D.; Kitano, T.; Ito, K. *Macromolecules* **1987**, *19*, 2533.
- (7) Pant, B. B.; Skolnick, J.; Yaris, R. *Macromolecules* **1985**, *18*, 253.
- (8) Weber, T. A.; Helfand, E. *J. Phys. Chem.* **1983**, *87*, 1881.

## Lattice Models of Branched Polymers: Dynamics of Uniform Stars

M. K. Wilkinson,\*† D. S. Gaunt,† J. E. G. Lipson,† and S. G. Whittington§

*Department of Physics, King's College, Strand, London WC2R2LS, U.K., Department of Chemistry, University of Guelph, Guelph, Ontario, Canada, and Department of Chemistry, University of Toronto, Toronto, Ontario, Canada. Received August 20, 1987; Revised Manuscript Received November 9, 1987*

**ABSTRACT:** We report exact enumeration and Monte Carlo results on the dynamics of uniform star polymers. The treatment is at the level of the Zimm rigid body approximation and we use a lattice model incorporating the effects of excluded volume. We have calculated the sedimentation velocity and intrinsic viscosity, and hence the hydrodynamic radius, as a function of the number of branches in the star and the number of monomers in each branch. We have varied the bare friction by changing the effective bead radius ( $a$ ) and we discuss the sensitivity of the results to the value of  $a$ . We compare our results, for appropriate ratios of quantities for branched and linear polymers, with those of other theoretical treatments and with experimental results.

### 1. Introduction

In 1980, Zimm<sup>1</sup> introduced a method for calculating dynamical properties of dilute polymer solutions by treating each conformation of the polymer as a rigid body, solving the hydrodynamic equations for each such rigid conformation, and averaging over a Monte Carlo sample of the conformations. This approach avoids solving the Kirkwood diffusion equation. It does not use the preaveraging approximation involved in the Kirkwood-Riseman treatment<sup>2</sup> but is, in itself, an approximation.<sup>3</sup> However, Wilemski and Tanaka<sup>4</sup> and Fixman have shown that Zimm's method yields bounds on the intrinsic viscosity and on the sedimentation coefficient.

Zimm's original calculations<sup>1</sup> were for Gaussian chains but the method has also been applied to "wormlike"<sup>5</sup> and Gaussian<sup>5,6</sup> models of uniform star polymers without excluded volume. Zimm<sup>7</sup> has also compared dynamic properties of uniform stars, with and without excluded volume.

All of the above calculations have been carried out for continuum models. In this paper we apply similar methods to lattice models of chains (i.e., to self-avoiding walks) and uniform stars, with excluded volume. The advantages of a lattice model are that, for a given amount of computer time, improved statistics can be obtained and, for small systems, enumeration methods can be used so that the averaging over conformations is exact. We have estab-

lished elsewhere<sup>8</sup> that the lattice dependence of certain quantities can be removed by taking appropriate ratios and that these ratios can be successfully compared with experiment.<sup>8,9</sup>

We study the sedimentation velocity ( $u$ ), and hence the corresponding hydrodynamic radius ( $R_h$ ), and the intrinsic viscosity ( $[\eta]$ ) for chains and for stars with  $f$  branches ( $f = 3-6$ ) on the simple cubic lattice. If each branch has  $n$  monomers, the total number ( $N$ ) of monomers is  $N = 1 + nf$ . For small  $N$ , we have calculated  $u$  and  $[\eta]$  exactly, within the Zimm algorithm, by enumerating all conformations, and we have extended these results to larger  $N$  (less than about 60) by an inversely restricted Monte Carlo method.<sup>10,11</sup> Sample sizes used were typically 5000 configurations. We have investigated the asymptotic behavior (large  $N$ ) of these quantities as a function of  $f$  and of the "bead" radius ( $a$ ). We compare our results for the viscosity ratio ( $g'$ ) and the ratio ( $h$ ) of the sedimentation rates with the Kirkwood<sup>2</sup> approximation and with previous theoretical and experimental results.

### 2. Sedimentation Velocity and Hydrodynamic Radius

The basic idea behind Zimm's approach<sup>1</sup> is to neglect coupling between small scale and center of mass motions. Consequently, each conformation is treated as a rigid body, the hydrodynamic equations are solved for the motion of this rigid body, and quantities such as the sedimentation velocity are calculated for each conformation. Finally, these quantities are averaged over all, or a sample of, the conformations of the molecule.

\* King's College.

† University of Guelph.

§ University of Toronto.

Table I  
Sedimentation Velocity  $u_z$  as a Function of  $f$ ,  $N$ , and  $a^a$

| $N$ | $a = 1/2$       |                 | $a = 1/4$       |                 |
|-----|-----------------|-----------------|-----------------|-----------------|
|     | $f = 1$         | $f = 3$         | $f = 1$         | $f = 3$         |
| 4   | 0.23165         | 0.23109         | 0.33993         | 0.34126         |
| 7   | 0.30881         | 0.31405         | 0.42055         | 0.42792         |
| 10  | 0.3688 ± 0.0003 | 0.37564         | 0.4832 ± 0.0004 | 0.49307         |
| 13  | 0.4189 ± 0.0004 | 0.4285 ± 0.0003 | 0.5354 ± 0.0004 | 0.5485 ± 0.0003 |
| 16  | 0.4626 ± 0.0003 | 0.4735 ± 0.0004 | 0.5807 ± 0.0005 | 0.5955 ± 0.0004 |
| 19  | 0.5023 ± 0.0003 | 0.5149 ± 0.0004 | 0.6214 ± 0.0005 | 0.6385 ± 0.0005 |
| 25  | 0.5710 ± 0.0004 | 0.5853 ± 0.0003 | 0.6926 ± 0.0006 | 0.7114 ± 0.0005 |
| 31  | 0.6310 ± 0.0004 | 0.6474 ± 0.0004 | 0.7544 ± 0.0006 | 0.7762 ± 0.0006 |
| 37  | 0.6847 ± 0.0007 | 0.7027 ± 0.0006 | 0.8100 ± 0.0007 | 0.8325 ± 0.0006 |
| 49  | 0.7778 ± 0.0007 | 0.7975 ± 0.0006 | 0.9056 ± 0.0008 | 0.9297 ± 0.0007 |
| 55  |                 |                 | 0.9482 ± 0.0009 | 0.9754 ± 0.0008 |

<sup>a</sup> Values without error bars were obtained by exact enumeration. The error bars represent one standard deviation.

Following Zimm,<sup>1</sup> we give a brief description of the relevant hydrodynamic equations. The molecule consists of  $N$  "beads", of radius  $a$ , at infinite dilution in a solution of viscosity  $\eta$  and we write  $\rho = 6\pi\eta a$ . The force on the  $i$ th bead is

$$\mathbf{F}_i = \rho(\mathbf{u}_i - \mathbf{v}_i) \quad (2.1)$$

where  $\mathbf{u}_i$  is the velocity of the  $i$ th bead and  $\mathbf{v}_i$  is the velocity which the fluid would have, at the location of the  $i$ th bead, in the absence of that bead. This fluid velocity can be written as the sum of the velocity ( $\mathbf{v}_i^0$ ) due to an externally imposed flow and that due to hydrodynamic interactions from the motion of all the other beads. That is

$$\mathbf{v}_i = \mathbf{v}_i^0 + \sum_{j \neq i} \mathbf{T}_{ij} \mathbf{F}_j \quad (2.2)$$

where  $\mathbf{T}_{ij}$  is the hydrodynamic interaction tensor. The familiar Oseen approximation for  $\mathbf{T}_{ij}$  is valid only at large distances and it is necessary to include correction terms. If  $r_{ij}$  is the distance between the  $i$ th and  $j$ th beads, one can expand<sup>12,13</sup>  $\mathbf{T}_{ij}$  in inverse powers of  $(r_{ij}/a)$ . The classical Oseen result is the zeroth term in this expansion. We include the term in  $(r_{ij}/a)^{-2}$  and note<sup>13</sup> that the next nonzero term is  $\mathcal{O}((r_{ij}/a)^{-6})$ . (In fact, Felderhof's calculations<sup>13</sup> are for freely rotating spheres but this is unlikely to make a major quantitative difference.)

Equations 2.1 and 2.2 give

$$\rho^{-1} \mathbf{F}_i + \sum_{j \neq i} \mathbf{T}_{ij} \mathbf{F}_j - \mathbf{u}_i = -\mathbf{v}_i^0 \quad (2.3)$$

which represents  $3N$  equations in  $6N$  unknowns (the forces and particle velocities). Supplementary conditions are used with eq 2.3, depending on the problem. In sedimentation one must consider the rotation of the molecule about the direction of the sedimenting force, which we assume to be in direction  $\mathbf{d}$  (not necessarily along a lattice axis). If  $\mathbf{u}$  is the velocity of the center of mass,  $\mathbf{u}_i$  can be written as

$$\mathbf{u}_i = \mathbf{u} + \boldsymbol{\Omega} \times \mathbf{r}_i \quad (2.4)$$

where  $\mathbf{r}_i$  is the position of the  $i$ th bead in the center of mass coordinate system and  $\boldsymbol{\Omega}$  is the angular velocity. This gives  $3N$  additional equations and four additional unknowns ( $\mathbf{u}$  and  $|\boldsymbol{\Omega}|$ ). The sedimenting force per bead is taken to be unity, so that

$$\sum_{i=1}^N \mathbf{F}_i = N\mathbf{d} \quad (2.5)$$

Moreover, since there is no torque about the  $\mathbf{d}$ -direction,

$$\mathbf{d} \cdot (\sum_i \mathbf{r}_i \times \mathbf{F}_i) = 0 \quad (2.6)$$

Equations 2.5 and 2.6 supply four additional equations without introducing any additional unknowns. In addition,  $\mathbf{v}_i^0$  is zero.

We can obtain the sedimentation velocity  $\mathbf{u}$  by solving the above set of  $6N + 4$  simultaneous linear equations. The hydrodynamic radius  $R_s$  is then given by

$$R_s = N/6\pi\eta_0 u_d \quad (2.7)$$

where  $\eta_0$  is the solvent viscosity, taken to be unity in the numerical calculations, and  $u_d = |\mathbf{u}|$ .

We now turn to our numerical results for chains and stars on the simple cubic lattice. A difficulty with a lattice model would arise if the results were sensitive to the direction of the sedimenting field, with respect to the lattice directions. We have checked that this effect is small by calculating the sedimentation velocity as a function of the polar angles  $\theta$  and  $\phi$ , defined with respect to the lattice directions. The isometries of the lattice are known<sup>14</sup> to be less important for longer chains and we have therefore carried out this calculation for a chain of three beads with  $a = 1/2$ , assuming unit lattice spacing. The calculated value of  $u(\theta, \phi)$  was 0.198016 for  $\theta = \phi = 0$  and 0.198028 for  $\theta = \phi = \pi/4$ . The velocities for other angles investigated lay between these limits and we conclude that the effect is negligible. Consequently, all our other calculations have been carried out with the sedimenting field along the  $z$ -axis.

In Table I we give our values of the sedimentation velocity  $u_z$  for  $a = 1/4$  and  $1/2$ ,  $f = 1$  and 3, for various values of  $N$ . As expected, the sedimentation velocity decreases as  $a$  increases (since the bare friction increases) and increases as  $f$  increases (since stars become more compact<sup>7,9</sup> for larger  $f$ ). We can convert  $u_z$  into an effective hydrodynamic radius,  $R_s = N/6\pi u_z$ , and we expect  $R_s$  to scale as  $N^\nu$  for large  $N$ . Anticipating the usual form<sup>15</sup> of confluent singularity, we plot  $R_s/N^\nu$  against  $N^{-\Delta}$  in Figure 1, with  $\nu = 0.588$  and  $\Delta = 0.47$ . The behavior is quite linear for each value of  $f$  and for both values of  $a$ . As expected, the hydrodynamic radius decreases smoothly as  $f$  increases and is larger (for given  $f$  and  $N$ ) for  $a = 1/2$  than for  $a = 1/4$ .

Defining the amplitude

$$A_s(f, a) = \lim_{N \rightarrow \infty} R_s/N^\nu \quad (2.8)$$

we note that, for given  $a$ ,  $A_s(f, a)$  decreases as  $f$  increases. For given  $f$ , there is some evidence that the amplitude is  $a$  dependent, being smaller for  $a = 1/4$  than for  $a = 1/2$ . It is also interesting to notice that the correction to scaling terms is larger for larger  $a$ , as evidenced by the (numerically) larger slopes of the corresponding curves in Figure 1.

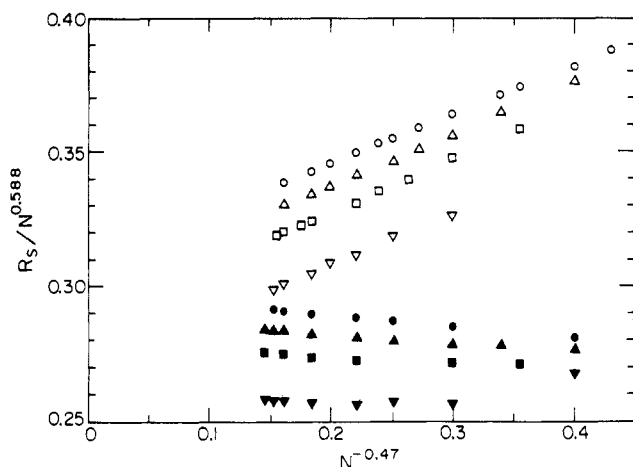


**Figure 1.** Scaled hydrodynamic radius plotted against  $N^{-0.47}$  for  $f=1$  (○),  $f=3$  (△),  $f=4$  (□), and  $f=6$  (▽) and for  $a=1/4$  (filled symbols) and  $a=1/2$  (open symbols).

**Table II**  
Comparison of Estimates of  $h$

|                                                                     | $f=3$             | $f=4$             | $f=6$             |
|---------------------------------------------------------------------|-------------------|-------------------|-------------------|
| $N=49, a=1/2$                                                       | $0.975 \pm 0.002$ | $0.946 \pm 0.002$ | $0.887 \pm 0.002$ |
| $N=49, a=1/4$                                                       | $0.974 \pm 0.002$ | $0.944 \pm 0.002$ | $0.884 \pm 0.002$ |
| Zimm, <sup>7</sup> $N=49$ with excluded volume                      |                   | $0.935 \pm 0.012$ | $0.887 \pm 0.010$ |
| Zimm, <sup>7</sup> $N=49$ without excluded volume                   |                   | $0.948 \pm 0.018$ | $0.895 \pm 0.017$ |
| Stockmayer and Fixman, <sup>18</sup> Gaussian stars                 | 0.947             | 0.892             | 0.798             |
| Kirkwood-Riseman <sup>5,19</sup> exptl (good solvent) <sup>17</sup> |                   | 0.91              | 0.86              |
| exptl ( $\theta$ solvent) <sup>17</sup>                             | 0.92–0.97         |                   |                   |
|                                                                     | 0.93–0.99         |                   |                   |

For comparison, we have calculated the hydrodynamic radius using the Kirkwood approximation<sup>16</sup>

$$1/R_s^K = 1/Na + \sum_{\substack{ij=1 \\ i \neq j}}^N \langle 1/r_{ij} \rangle / N^2 \quad (2.9)$$

Using  $a=1/2$  as an example, we plot  $R_s^K(3)/N^{0.588}$  against  $N^{-0.47}$  in Figure 2. For comparison, we give the corresponding "hydrodynamic" results, with no "free draining" contribution. In this case, we know from (2.9) that these two curves must extrapolate to the same value  $A_s^K(3)$ . We also show the corresponding data for the Zimm approximation for  $a=1/2$  in the same figure. It is clear from inspection of this figure that  $A_s(3, 1/2) > A_s^K(3)$  and this result is also found for other values of  $f$ .

Our experience<sup>8,9</sup> with equilibrium properties, such as the mean-square radius of gyration, suggests that we can remove the lattice dependence by taking ratios such as  $h = R_s(f)/R_s(1)$ , i.e., by measuring the dimensions of the star in reduced units, relative to the linear molecule with the

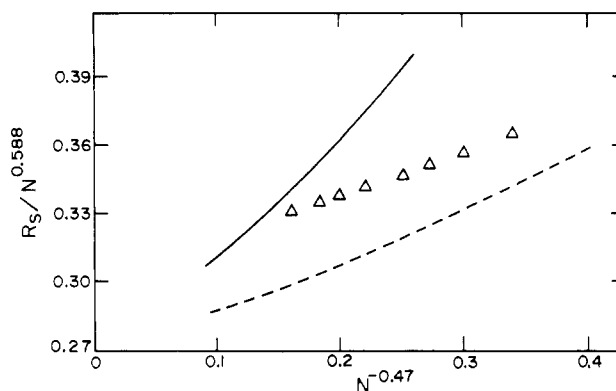


**Figure 2.** Scaled hydrodynamic radius plotted against  $N^{-0.47}$ , for  $f=3$ . The full curve is the hydrodynamic contribution to the Kirkwood approximation; the broken curve includes the bare friction in the Kirkwood approximation for  $a=1/2$ . The triangles are the values in the Zimm approximation for  $a=1/2$ .

same degree of polymerization. In Table II we give our estimated values of  $h$  for  $f=3-6$ ,  $N=49$ ,  $a=1/2$ , and  $a=1/4$  and compare these values both with similar results by Zimm,<sup>7</sup> which incorporate excluded volume effects, with other theoretical treatments,<sup>5,18,19</sup> and with some experimental results.<sup>17</sup>

We find that, at  $N=49$ , the value of  $h$  is essentially independent of  $a$  for all values of  $f$  considered here. Our values of  $h$  agree with those calculated by Zimm<sup>7</sup> to within the uncertainties, which reflects the fact that reduced quantities (such as  $h$ ) are effectively lattice independent. However, our error bars are considerably smaller than Zimm's, reflecting (in part) our much larger sample sizes.

### 3. Intrinsic Viscosity

The Zimm algorithm can also be used to calculate the intrinsic viscosity. Equation 2.3 is used together with the constraint

$$\sum_i \mathbf{F}_i = 0 \quad (3.1)$$

Since each bead moves with the center of mass velocity ( $\mathbf{u}_i = \mathbf{u}$ ) we have  $3N+3$  equations in  $3N+3$  unknowns (the forces and  $\mathbf{u}$ ). In this case the externally applied velocity field  $\{\mathbf{v}_i^0\}$  is taken to be the irrotational part of a simple laminar flow. For example, one can take  $\mathbf{v}_i^0 = (z_i, 0, x_i)$  where  $x_i$  and  $z_i$  refer to the coordinates in the center of mass system.

Following Zimm we calculate the dimensionless quantity  $E$ ,

$$E = \sum_i (z_i F_{ix} + x_i F_{iz}) / 2N \quad (3.2)$$

which is proportional to  $[\eta]$ , the intrinsic viscosity. The two terms in brackets correspond to two equivalent choices

**Table III**  
Estimates of  $E$  for  $f=1, 3$ , and  $6$  and  $a=1/4$  and  $1/2^a$

| $N$ | $a=1/4$          |                  |                 | $a=1/2$          |                  |                  |
|-----|------------------|------------------|-----------------|------------------|------------------|------------------|
|     | $f=1$            | $f=3$            | $f=6$           | $f=1$            | $f=3$            | $f=6$            |
| 4   | 1.2758           | 1.1971           |                 | 3.0334           | 3.0498           |                  |
| 7   | 2.3106           | 2.0124           | 1.7240          | 4.6983           | 4.3160           | 4.4449           |
| 10  | $3.28 \pm 0.05$  | 2.7961           |                 | $6.09 \pm 0.07$  | 5.4581           |                  |
| 13  | $4.17 \pm 0.06$  | $3.49 \pm 0.04$  | $2.47 \pm 0.01$ | $7.30 \pm 0.09$  | $6.39 \pm 0.06$  | $4.94 \pm 0.01$  |
| 19  | $5.94 \pm 0.08$  | $4.84 \pm 0.05$  | $3.38 \pm 0.01$ | $9.64 \pm 0.12$  | $8.18 \pm 0.08$  | $6.17 \pm 0.02$  |
| 25  | $7.50 \pm 0.05$  | $6.27 \pm 0.03$  | $4.15 \pm 0.01$ | $11.57 \pm 0.05$ | $10.00 \pm 0.03$ | $7.12 \pm 0.02$  |
| 37  | $10.28 \pm 0.07$ | $8.73 \pm 0.04$  | $5.66 \pm 0.02$ | $15.12 \pm 0.07$ | $13.00 \pm 0.04$ | $9.08 \pm 0.02$  |
| 49  | $13.13 \pm 0.09$ | $11.12 \pm 0.06$ | $7.18 \pm 0.02$ | $18.48 \pm 0.08$ | $15.95 \pm 0.06$ | $10.97 \pm 0.02$ |
| 61  | $15.93 \pm 0.10$ | $13.20 \pm 0.07$ | $8.54 \pm 0.03$ | $21.75 \pm 0.15$ | $18.49 \pm 0.09$ | $12.57 \pm 0.04$ |

<sup>a</sup> Values without error bars were obtained by exact enumeration. The error bars represent one standard deviation.

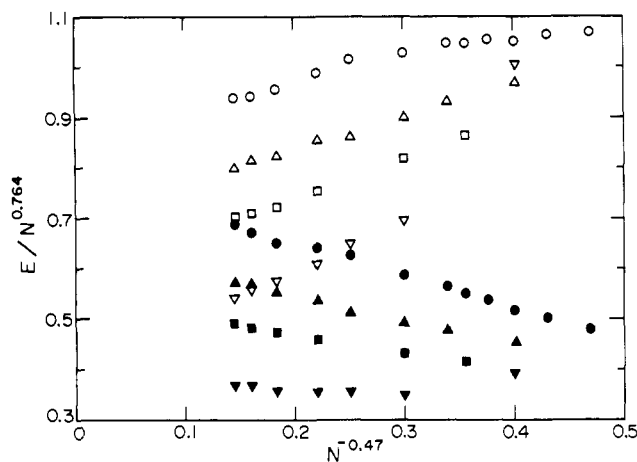


**Figure 3.** Reduced intrinsic viscosity plotted against  $N^{-0.47}$  for  $f = 1$  (○),  $f = 3$  (Δ),  $f = 4$  (□), and  $f = 6$  (▽) and for  $a = 1/4$  (filled symbols) and  $a = 1/2$  (open symbols).

**Table IV**  
Comparison of Estimates of  $g'$

|                                                     | $f = 3$           | $f = 4$           | $f = 6$           |
|-----------------------------------------------------|-------------------|-------------------|-------------------|
| $N = 49, a = 1/2$                                   | $0.863 \pm 0.007$ | $0.749 \pm 0.005$ | $0.594 \pm 0.004$ |
| $N = 49, a = 1/4$                                   | $0.847 \pm 0.010$ | $0.716 \pm 0.008$ | $0.547 \pm 0.005$ |
| Zimm, <sup>7</sup> $N = 49$ with excluded volume    |                   | $0.734 \pm 0.034$ | $0.563 \pm 0.020$ |
| Zimm, <sup>7</sup> $N = 49$ without excluded volume |                   | $0.713 \pm 0.056$ | $0.580 \pm 0.041$ |
| Freire et al. <sup>5</sup> ( $\theta$ conditions)   |                   |                   | $0.59 \pm 0.02$   |
| Freire et al. <sup>21</sup> (good solvent)          |                   |                   | $0.584 \pm 0.008$ |
| Stockmayer and Fixman <sup>18</sup>                 | 0.8501            | 0.7093            | 0.5074            |
| exptl <sup>17,22,23</sup> (good solvent)            | 0.88–0.90         | 0.72–0.84         | 0.57–0.58         |
| exptl <sup>17,22,23</sup> ( $\theta$ solvent)       | 0.83–0.94         | 0.75–0.82         | 0.62–0.63         |

of flow field and are averaged in order to improve the statistics. In Table III we give our values of  $E$  for  $a = 1/4$  and  $1/2$ ,  $f = 1, 3$ , and  $6$ , for various values of  $N$ . As in the sedimentation case the value of  $E$  increases for increasing bead radius because the "bare friction" is increased. The effect of increasing  $f$  is to reduce the effective radius of the molecule (for given  $N$ ) and therefore to reduce the viscosity.

From scaling arguments<sup>20</sup> one would expect for large  $N$  that

$$E \sim R_{\eta}^3/N \quad (3.3)$$

where  $R_{\eta}$  is a hydrodynamic radius defined in terms of viscosity. General universality considerations imply that  $R_{\eta} \sim N^{\nu}$ , and we have analyzed the data by assuming that  $\nu = 0.588$ . We plot  $E/N^{3\nu-1}$  against  $1/N^{0.47}$  in Figure 3 for  $f = 1, 3, 4$ , and  $6$ ,  $a = 1/2$  and  $1/4$ . For each value of  $f$  the curves for different values of  $a$  appear to have different intercepts. We shall discuss this point in the concluding section.

As in the previous section we compare our lattice results with continuum theoretical and experimental results by considering ratios. The appropriate quantity here is  $g'(f) = [\eta]_f/[\eta]_1 = E(f)/E(1)$  and we compare our estimates for  $N = 49$  with other results in Table IV. Zimm's calculated values of  $g'$  lie between our estimates with  $a = 1/4$  and  $a = 1/2$ , both for  $f = 4$  and  $f = 6$ . The experimental values are scattered over a wide range but there is general agreement between them and our results.

Unlike the results for  $h$ , our estimates of  $g'$  at  $N = 49$  seem to be  $a$ -dependent and the differences at  $a = 1/4$  and  $a = 1/2$  become more marked as  $f$  increases. In order to

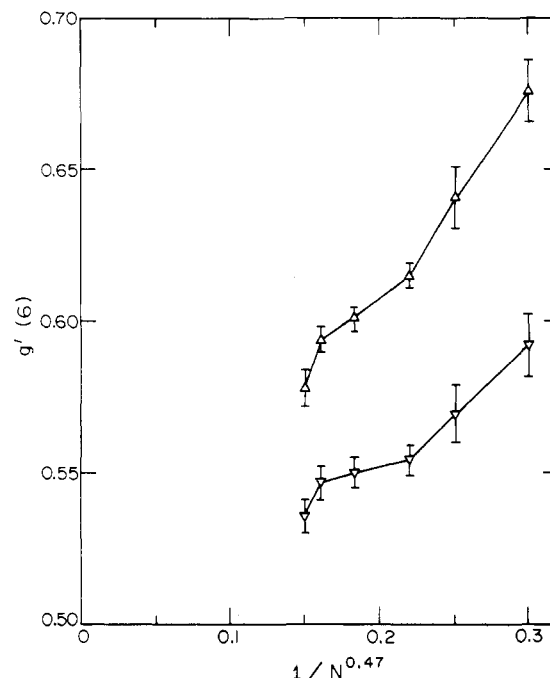


**Figure 4.**  $N$  dependence of the viscosity ratio for  $f = 6$ , when  $a = 1/4$  (▽) and when  $a = 1/2$  (Δ).

investigate whether this  $a$  dependence persists for large  $N$  we have plotted  $g'$  against  $N^{-0.47}$  in Figure 4. The values of  $g'$  for  $a = 1/4$  and  $a = 1/2$  become closer as  $N$  increases and there is no evidence that the  $a$  dependence persists in the  $N \rightarrow \infty$  limit.

#### 4. Discussion

In previous papers we have used a lattice model to study the static behavior of polymers in dilute solution. The present work is an application of the model to dynamical problems. Using Zimm's rigid body algorithm we have calculated values, in three dimensions, for the sedimentation velocity and intrinsic viscosity for uniform stars with 1–6 branches. Our experience with related equilibrium problems leads us to expect that lattice effects are removed by considering suitable ratios of quantities (e.g.,  $h$  and  $g'$  in Tables II and IV). The agreement which we find with Zimm's continuum model confirms this view and such numerical calculations can therefore be compared with experimental results. The advantage of a lattice model, as opposed to a continuum model, is that very much smaller error bars are obtainable for a given amount of computational effort.

The qualitative dependence of the dynamical quantities on  $f$  and  $N$  is what one would intuitively expect. Where our results can be compared with existing quantitative results, the agreement is very good. We conclude from Figures 1 and 3 that in order to have any quantitative success in extrapolating to very large polymers, one must adequately take into account correction-to-scaling terms. Note that the Gaussian<sup>5,7</sup> values for  $h$  and  $g'$  are close to the experimental values for both good and  $\theta$  solvents and to our own work which incorporates excluded volume. We conclude that, as for static properties, solvent quality is rather unimportant when considering such ratios.

Our calculations have been carried out for two values of the bead radius (and hence for two values of the bare friction). The sedimentation velocity and intrinsic viscosity depend on the value of this radius for small  $N$ . To investigate the large  $N$  behavior we have defined amplitudes (e.g., eq 2.8) and examined their possible dependence on  $a$ . Our results suggest a weak  $a$  dependence both in the

case of sedimentation and viscosity. The corresponding amplitudes in the Kirkwood approximation do not depend on  $a$  since the hydrodynamic terms dominate the bare friction in eq 2.9. This raises the question of whether  $a$ -dependent amplitudes are reasonable. The approximation which we have used for the hydrodynamic  $T$  matrix goes beyond the Oseen approximation and incorporates  $a$ -dependent off-diagonal terms. Hence, even though these terms will dominate the diagonal (bare friction) terms for large  $N$ , their  $a$  dependence may be reflected in  $a$ -dependent amplitudes. Indeed, quite generally in critical phenomena, although critical exponents are not normally sensitive to local properties, critical amplitudes usually are. Fixman has also suggested that there is a nonuniversal dependence of limiting quantities on "local" properties. His conclusions are based on dynamical simulations,<sup>24</sup> equilibrium simulations,<sup>25</sup> and simulations involving internal friction.<sup>26</sup> This apparent dependence is worthy of further investigation.

**Acknowledgment.** This research was financially supported, in part, by NSERC, by SERC, and by NATO (Grant RG85/0067). We acknowledge helpful conversations with Professor Raymond Kapral.

## References and Notes

- (1) Zimm, B. H. *Macromolecules* **1980**, *13*, 592.
- (2) See, for instance: Yamakawa, H. *Modern Theory of Polymer Solutions*; Harper and Row: New York, 1971; Chapter 6.
- (3) Fixman, M. *Macromolecules* **1981**, *14*, 1706. Zimm, B. H. *Macromolecules* **1982**, *15*, 520.
- (4) Wilemski, G.; Tanaka, G. *Macromolecules* **1981**, *14*, 1531. Fixman, M. *J. Chem. Phys.* **1983**, *78*, 1588.
- (5) Zimm, B. H. *Macromolecules* **1984**, *17*, 795.
- (6) Freire, J. J.; Prats, R.; Pla, J.; de la Torre, J. G. *Macromolecules* **1984**, *17*, 1815.
- (7) Zimm, B. H. *Macromolecules* **1984**, *17*, 2441.
- (8) Lipson, J. E. G.; Gaunt, D. S.; Wilkinson, M. K.; Whittington, S. G. *Macromolecules* **1987**, *20*, 186.
- (9) Whittington, S. G.; Lipson, J. E. G.; Wilkinson, M. K.; Gaunt, D. S. *Macromolecules* **1986**, *19*, 1241.
- (10) Rosenbluth, A. W.; Rosenbluth, M. N. *J. Chem. Phys.* **1955**, *23*, 356.
- (11) Hammersley, J. M.; Morton, K. W. *J. Roy. Statist. Soc.* **1954**, *B16*, 23.
- (12) Rotne, J.; Prager, S. *J. Chem. Phys.* **1969**, *50*, 4831.
- (13) Felderhof, B. U. *Physica A (Amsterdam)* **1977**, *89A*, 373.
- (14) Domb, C.; Gillis, J.; Wilmers, G. *Proc. Phys. Soc.* **1965**, *85*, 625.
- (15) LeGuillou, J. C.; Zinn-Justin, J. *Phys. Rev. B: Condens. Matter* **1980**, *21*, 3976.
- (16) Kirkwood, J. G. *J. Polym. Sci.* **1954**, *12*, 1.
- (17) Huber, K.; Burchard, W.; Fetters, L. J. *Macromolecules* **1984**, *17*, 541.
- (18) Stockmayer, W. H.; Fixman, M. *Ann. N. Y. Acad. Sci.* **1953**, *57*, 334.
- (19) Prats, R.; Pla, J.; Friere, J. J. *Macromolecules* **1983**, *16*, 1701.
- (20) de Gennes, P.-G. *Scaling Concepts in Polymer Physics*; Cornell University Press: Ithaca, NY, 1979.
- (21) Rey, A.; Freire, J. J.; de la Torre, J. G. *Macromolecules* **1987**, *20*, 342.
- (22) Roovers, J. E. L.; Bywater, S. *Macromolecules* **1972**, *5*, 384; **1974**, *7*, 443.
- (23) Hadjichristidis, N.; Roovers, J. E. L. *J. Polym. Sci., Polym. Phys. Ed.* **1974**, *12*, 2521.
- (24) Fixman, M. *Macromolecules* **1981**, *14*, 1710; *J. Chem. Phys.* **1983**, *78*, 1594.
- (25) Fixman, M. *J. Chem. Phys.* **1986**, *84*, 4080.
- (26) Fixman, M. *J. Chem. Phys.* **1986**, *84*, 4085.

## Attraction between Lipid Bilayer Membranes in Concentrated Solutions of Nonadsorbing Polymers: Comparison of Mean-Field Theory with Measurements of Adhesion Energy

E. Evans\* and D. Needham†

*Departments of Pathology & Physics, University of British Columbia, Vancouver, B.C., Canada V6T 1W5, and Department of Mechanical Engineering and Material Science, Duke University, Durham, North Carolina 27706. Received February 19, 1987*

**ABSTRACT:** Recent experimental advances have made quantitation of weak membrane attraction possible in concentrated solutions of macromolecules. Here, we report direct measurements of the free energy potential for adhesion of synthetic lipid bilayers in aqueous solutions of dextran (polyglucose) over a wide range of volume fraction (0.01–0.1) and molecular weight (10 000–150 000). These polymer solutions are well-modeled by a Flory interaction parameter of 0.43, characteristic of a "good" solvent. Controlled assembly of two giant bilayer vesicles was used to evaluate the free energy potential for formation of adhesive contact. The adhesion energy for neutral (phosphatidylcholine) bilayers in 0.1 M NaCl was found to steadily increase (from 0.01 to  $>0.2$  erg/cm<sup>2</sup>) with polymer volume fraction—without any indication of a plateau—and with little dependence of polymer size. The distance dependence of the polymer-induced field was tested by incorporation of electric (phosphatidylserine) charges in the lipid bilayer surfaces to stabilize adhesion at larger membrane separations. With the use of fluorescently labeled polymer, attempts were made to measure the concentration of polymer in the gap between adherent neutral bilayers; the result was negative, which indicated a significant reduction between the surfaces. Hence, we examined a thermodynamic mean-field theory for adhesion based on interaction of surface-depletion layers. Our analysis shows that (for equilibrium exchange of the polymer between gap and bulk regions) the attractive stress on the membrane surfaces is simply the osmotic pressure reduction at the midpoint of the gap relative to the bulk region. Calculations of adhesion energies based on the mean-field theory agree very well with the concentration dependence of neutral bilayer adhesion for large molecular weights and with the attenuation of adhesion energy due to electric double-layer repulsion between charged bilayers in polymer solutions fixed at a specific concentration.

## Introduction

Processes that cause aggregation of cells and other membrane-bound capsules in solutions of large macro-

molecules are generally separated into two categories: specific and nonspecific. Specific adhesion processes involve identifiable binding reactions between suspended macromolecules and receptor molecules located at the membrane surfaces. On the other hand, nonspecific adhesion processes are not attributable to cross-binding of membrane surfaces by the suspended macromolecules.

\*To whom correspondence should be sent at the University of British Columbia.

†Duke University.